

Topological Alterations and Symptom-Relevant Modules in the Whole-Brain Structural Network in Semantic Dementia

Junhua Ding^{a,1}, Keliang Chen^{b,1}, Weibin Zhang^c, Ming Li^c, Yan Chen^a, Qing Yang^b, Yingru Lv^d, Qihao Guo^{b,*} and Zaizhu Han^{a,*}

^aState Key Laboratory of Cognitive Neuroscience and Learning & IDG/McGovern Institute for Brain Research, Beijing Normal University, Beijing, China

^bDepartment of Neurology, Huashan Hospital, Fudan University, Shanghai, China

^cDepartment of Psychology, Beijing Normal University, Beijing, China

^dDepartment of Radiology, Huashan Hospital, Fudan University, Shanghai, China

Handling Associate Editor: Sharon Savage

Accepted 14 June 2017

Abstract.

Background: Semantic dementia (SD) is characterized by a selective decline in semantic processing. Although the neuropsychological pattern of this disease has been identified, its topological global alterations and symptom-relevant modules in the whole-brain anatomical network have not been fully elucidated.

Objective: This study aims to explore the topological alteration of anatomical network in SD and reveal the modules associated with semantic deficits in this disease.

Methods: We first constructed the whole-brain white-matter networks of 20 healthy controls and 19 patients with SD. Then, the network metrics of graph theory were compared between these two groups. Finally, we separated the network of SD patients into different modules and correlated the structural integrity of each module with the severity of the semantic deficits across patients.

Results: The network of the SD patients presented a significantly reduced global efficiency, indicating that the long-distance connections were damaged. The network was divided into the following four distinctive modules: the left temporal/occipital/parietal, frontal, right temporal/occipital, and frontal/parietal modules. The first two modules were associated with the semantic deficits of SD.

Conclusion: These findings illustrate the skeleton of the neuroanatomical network of SD patients and highlight the key role of the left temporal/occipital/parietal module and the left frontal module in semantic processing.

Keywords: Graph theoretical analysis, lesion-symptom mapping, network module, semantic deficit, semantic dementia, topological alteration, white-matter neural network

¹These authors contributed equally to this work.

*Correspondence to: Zaizhu Han, State Key Laboratory of Cognitive Neuroscience and Learning & IDG/McGovern Institute for Brain Research, Beijing Normal University, Beijing 100875,

China. Tel.: +86 10 58804690; E-mail: zzhhan@bnu.edu.cn. and Qihao Guo, Department of Neurology, Huashan Hospital, Fudan University, Shanghai, 200040, China. Tel.: +86 2152888162; E-mail: dr.guoqihao@126.com.

INTRODUCTION

Semantic memory is a pivotal cognitive component of the human brain and refers to general world knowledge about objects, people, words, and facts [1]. This memory system is selectively impaired in semantic dementia (SD), which is a progressive neurodegenerative disease. Patients with SD often show a gradual decline in semantic function regardless of modalities of inputs and outputs [2–5], with a relative sparing of other cognitive domains [6, 7]. Thus, this disease provides an ideal model to investigate the neural mechanism of semantic processing. Prior studies have observed that individuals with SD suffer from atrophy in multiple cerebral cortices [8, 9], functional, and structural pathways [10, 11]. However, most of the findings regarding networks have been derived from seed-based analyses and only obtained networks connected to the given seeds of SD [11–13]. For instance, Guo and colleagues [11] found that functional connectivity was decreased between the anterior temporal lobe (ATL) and other modality-specific areas in patients with SD. Similarly, structural changes were also found on the white-matter tracts connecting the ATL to other regions, such as the inferior longitudinal fasciculus, uncinate fasciculus, and inferior fronto-occipital fasciculus [6, 10, 14, 15].

While the literature has revealed a widely distributed network that is specific to semantic processing in normal subjects [16–19], previous seed-based studies in SD might only reveal a part of the network of SD. Thus, changes of the global network in SD are unknown. Recently, Agosta and colleagues [20] filled such a gap by investigating the graph theoretical measures (e.g., network degree, global efficiency, local efficiency, and assortativity) of the global network in SD using resting-state functional magnetic resonance imaging (MRI) data. The authors found that compared to healthy controls, SD patients had lower values in network degree, and global and local efficiency, and higher value in assortativity. However, it is unclear whether this functional global network in SD has a corresponding anatomical basis.

More importantly, the human brain network is intrinsically composed of distinctive modules [21], and each module subserves a specific function [22]. Farb and colleagues [23] found that the functional abnormality in SD was mainly distributed in three following modules: salience, executive, and default mode ones. Since the relationship between modu-

lar pathology and semantic symptom has not been investigated, it is unknown which modules are associated with the semantic disruption in SD.

To characterize the topological global attributes of whole-brain white-matter networks in SD and identify which impaired modules cause the semantic disorder in SD, the current study collected diffusion-weighted images (DWI) and semantic performance data from 19 SD patients and 20 healthy controls. We first constructed the whole-brain structural networks of the two subject groups. Then, we calculated the global changes in the networks by comparing the graph-theoretical measures between the subject groups. Finally, we separated the SD network into different modules and acquired the semantic-relevant modules by correlating the integrity value of each module with the semantic performance of the SD patients (see Fig. 1). We assumed that the structural network in SD patients would have topological alteration relative to that of the healthy controls. Moreover, the modules, including regions in the left temporal lobe, could contribute to the semantic deterioration in SD.

MATERIALS AND METHODS

Participants

We recruited 19 adults with SD (12 males; mean age: 61.26 ± 8.63 y; mean education level: 11.53 ± 3.34 y; disease duration: 3.03 ± 1.46 y) and 20 healthy controls (8 males; mean age: 60.50 ± 3.93 y; mean education level: 10.45 ± 2.89 y) from Huashan Hospital in Shanghai. All participants were right-handed [24] native Chinese-speakers. The subject sample was the same as that in our recent study [25]. The participants underwent a set of comprehensive neuropsychological assessments. All patients satisfied the diagnostic criteria of SD [26], and presented selective dysfunction in semantic processing and atrophy in the ATL (see Table 1). This study was approved by the Institutional Review Board of the National Laboratory of Cognitive Neuroscience and Learning, Beijing Normal University.

Collection and preprocessing of neuropsychological data

The methods used to collect and preprocess the neuropsychological data in the present study have been previously elaborated by Ding et al. [25]. For

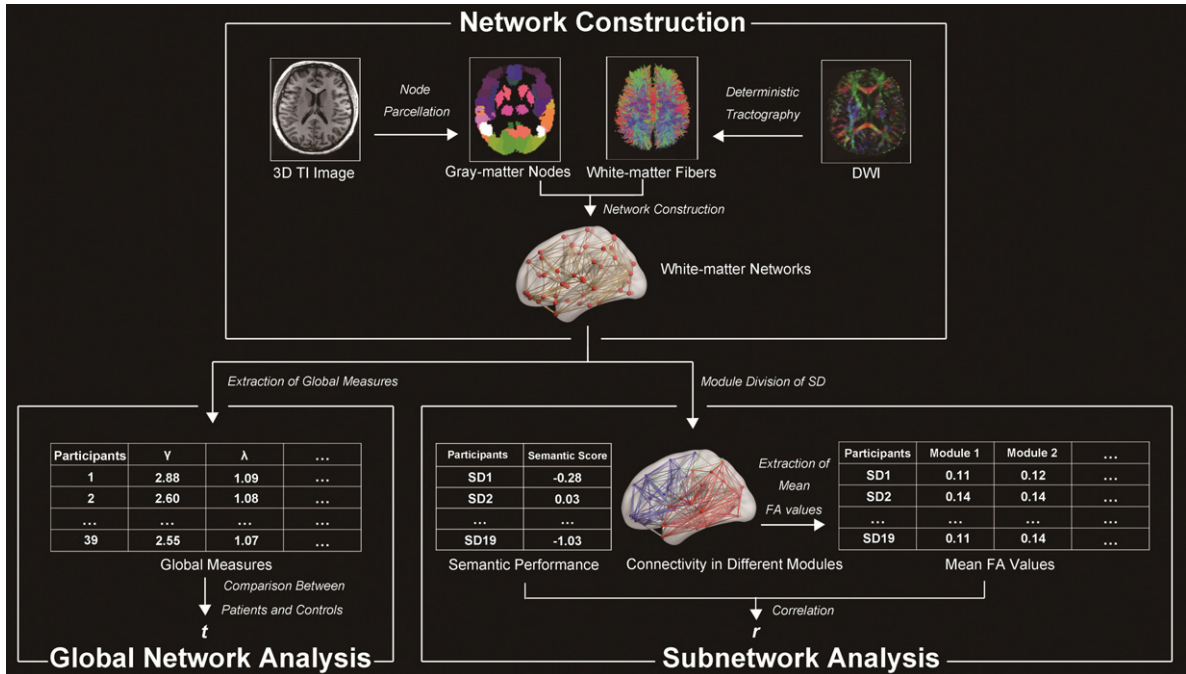


Fig. 1. Flowchart of the analyses performed in this study. NC, normal controls; SD, semantic dementia; DWI, diffusion-weighted images.

simplicity, these methods are not described in detail here.

Each subject was evaluated on the following three aspects of cognitive abilities. (1) *Semantic processing ability*. Semantic processing ability was assessed by the following six tasks: oral picture naming ($n = 140$; subjects were instructed to name the objects shown in pictures that appeared on a screen), oral sound naming ($n = 36$; subjects were instructed to name the objects that produced the sounds they heard), picture associative matching ($n = 70$; subjects were instructed to identify which of the two pictures of objects shown in the bottom was semantically closer to the top picture of the object that appeared on the screen), word associative matching ($n = 70$; this task is identical to the picture associative matching task except that the pictures were replaced with the corresponding written words), word-picture verification ($n = 70$; subjects were instructed to determine whether the object and the word on the screen were identical), and naming to definition ($n = 70$; subjects were instructed to name the objects whose definitions were visually and aurally presented). The tasks shared semantic components but varied in the modalities of the inputs and outputs. (2) *Non-semantic processing ability*. Non-semantic processing ability was evaluated by the following three tasks:

sound perception ($n = 44$; subjects were instructed to determine whether the episode of sound has the same rhythm and pitch), visual perception ($n = 30$; subjects were instructed to determine whether two circles were the same), and proximity judgment ($n = 3$; subjects were instructed to determine which of two numbers was quantitatively closer to a third number that appeared on a screen). These tasks required minimal semantic involvement. (3) *General cognitive ability* was measured using the Chinese version of the Mini-Mental State Examination (MMSE) [27].

To obtain the cognitive measures, we first calculated the accuracy of each subject on each task. Each patient's accuracy on each task was further corrected into a standardized t -score based on the distribution of scores of the healthy control group to rule out the influence of demographic variables. This method was developed by Crawford and Garthwaite [28] and has been widely adopted [25, 29, 30]. Specifically, a regression model was first established for each task in the normal control group, in which the accuracy of the task was treated as the dependent variable and the demographic factors (i.e., age, gender, and education level) were treated as predictors. Then, the predicted accuracy of a patient was acquired by adding his or her demographic factors into the

Table 1
Demographic and clinical information of participants

	Healthy controls	SD patients	
	Raw score	Raw score	Corrected <i>t</i> score
Demographic characteristics			
Age (years)	60.50 (3.93)	61.26 (8.63)	
Gender (male:female)	8:12	12:7	
Education level (years)	10.45 (2.89)	11.53 (3.34)	
Handedness (right:left)	20:0	19:0	
Disease duration (years)		3.03 (1.46)	
Neuropsychological performance			
<i>Semantic</i>			
Oral picture naming (<i>n</i> = 140)	89% (6%)	24% (15%)*	-10.26 (2.65)
Oral sound naming (<i>n</i> = 36)	71% (11%)	19% (12%)*	-4.30 (1.35)
Picture associative matching (<i>n</i> = 70)	95% (3%)	72% (11%)*	-5.39 (2.79)
Word associative matching (<i>n</i> = 70)	96% (2%)	70% (13%)*	-17.67 (9.78)
Word-picture verification (<i>n</i> = 70)	96% (3%)	57% (20%)*	-12.34 (6.82)
Naming to definition (<i>n</i> = 70)	83% (8%)	19% (17%)*	-10.05 (3.15)
<i>Language</i>			
Word reading (<i>n</i> = 24)	96% (5%)	67% (25%)*	-6.01 (5.34)
Sentence comprehension (<i>n</i> = 8)	93% (22%)	89% (14%)	0.13 (0.69)
Oral repetition (<i>n</i> = 12)	96% (8%)	92% (11%)	-0.44 (1.18)
<i>General cognitive state</i>			
MMSE (max = 30)	93% (5%)	68% (15%)*	-3.81 (2.21)
<i>Arithmetic</i>			
Proximity judgment (<i>n</i> = 3)	93% (14%)	84% (23%)	-0.46 (1.41)
<i>Perception</i>			
Sound perception (<i>n</i> = 44)	88% (10%)	76% (11%)*	-0.91 (0.90)
Visual form perception (<i>n</i> = 30)	91% (5%)	94% (14%)	0.45 (0.55)
<i>Episodic memory</i>			
REY-O recall (max = 36)	45% (18%)	25% (12%)*	-1.23 (1.16)
<i>Executive function</i>			
STT (seconds)	91 (36)	121 (75)	0.87 (2.09)
Cerebral gray matter volume			
whole brain (cm ³)	421 (28)	372 (39)*	-1.62 (1.16)
temporal pole (cm ³)			
Left temporal pole	5.09 (0.78)	1.35 (0.52)*	-3.92 (0.66)
Right temporal pole	6.62 (0.78)	2.90 (1.80)*	-4.27 (1.95)
Dominant atrophy (right:left)		6:13	

MMSE, Mini-Mental State Examination; STT, shape trail test; SD, semantic dementia. ***p* < 0.01, ****p* < 0.001.

model. The discrepancy value was further extracted by the observed accuracy minus the predicted accuracy. Finally, we calculated the standardized *t* score of patients, (i.e., the quotient of the discrepancy value divided by the corrected standard error of the estimate).

To obtain a semantic index that could reliably reflect the degree of the semantic deficits in the SD subjects, we conducted a principle component analysis (PCA) using the above-mentioned 6 semantic tasks and 3 non-semantic tasks from the 19 patients. We used subcommands for varimax rotation, a plot of eigenvalues (>1), and a principal components extraction. The factor with the highest loading weight on all six semantic tasks was considered as the semantic factor, and the scores corresponding to this factor were considered to reflect the semantic performance of the SD subjects.

Collection and preprocessing of neuroimaging data

Collection

Each subject was scanned to collect two types of data using a Siemens 3T scanner at Huashan Hospital in Shanghai. (1) *3D T1-weighted images*: These images were acquired in the sagittal plane using the following parameters: repetition time = 2300 ms, echo time = 2.98 ms, flip angle = 9°, matrix size = 240 × 256, field of view = 240 × 256 mm, slice number = 192 slices, slice thickness = 1 mm, and voxel size = 1 × 1 × 1 mm. (2) *Diffusion-weighted images*: These images were acquired in the transverse plane using the following parameters: repetition time = 8500 ms, echo time = 87 ms, flip angle = 90°, matrix size = 128 × 128, field of view = 230 × 230 mm, slice number = 42 slices, slice thickness = 3 mm,

voxel size = $1.8 \times 1.8 \times 3$ mm, and direction number = 20 directions. The sequence was scanned twice to improve the image quality.

Preprocessing

The T1 images in the native space were first resampled into the voxel size of $1.5 \times 1.5 \times 1.5$ mm and were segmented into different types of brain tissue, followed by spatial normalization to the Montreal Neurological Institute (MNI) space using SPM8 (<http://www.fil.ion.ucl.ac.uk/spm/>) on the gray-matter images. Then, gray-matter volume (GMV) images were generated via affine and non-linear transformation and were smoothed using an 8-mm full-width at half-maximum Gaussian kernel. The DWI data were preprocessed using a pipeline toolbox for analyzing brain diffusion images (PANDA) [31]. First, we performed brain extraction on the b0 images. Second, we corrected for the eddy-current distortion and simple head-motion by registering DWI to the b0 images with an affine transformation. Third, the tensor model was built in the native space. We calculated the following three diffusivities: one diffusivity was in the axial direction (λ_1) and the other two diffusivities were in the radial directions (λ_2 and λ_3). Using these diffusivities, we acquired four voxel-wise diffusion tensor metrics [32, 33], which reflect different profiles of the white matter integrity as follows [6]: fractional anisotropy (FA) $\left(\sqrt{\frac{3}{2}} * \sqrt{\frac{(\lambda_1 - \lambda_{\text{mean}})^2 + (\lambda_2 - \lambda_{\text{mean}})^2 + (\lambda_3 - \lambda_{\text{mean}})^2}{\lambda_1^2 + \lambda_2^2 + \lambda_3^2}} \right)$, mean diffusivity (MD, average of the three diffusivities), radial diffusivity (RD, average of λ_2 and λ_3), and axial diffusivity (AD, i.e., λ_1). Finally, we non-linearly registered the individual images in the native space to the template in the MNI space (voxel size: $2 \times 2 \times 2$ mm) for comparisons across subjects.

Construction of the networks in the SD and healthy subjects

We constructed whole-brain white-matter networks in the two subject groups using the following steps (see Fig. 1).

Defining the gray-matter nodes

For each subject, the gray-matter mask of the whole brain was first parcellated into 90 regions according to the automated anatomical labelling (AAL) atlas in the MNI space [34]. Then, the regions were transformed into the native space using PANDA (i.e., the images

were first coregistered to the T1 images. Then, the T1 image was normalized to the ICBM-152 template in the MNI space. Finally, the atlas was transformed into the native space using the above-mentioned transformation information; see similar methods in [35]). Thus, we obtained 90 gray-matter regions/nodes of each subject in the native space.

Tracking white-matter connections between gray-matter nodes

To identify the white-matter connections/edges among the 90 AAL regions/nodes in each subject, we first tracked the fibers in each subject's native space using a deterministic fiber-tracking program via the FACT tracking algorithm [36]. Fiber tracing between voxels was performed and terminated when the angle between two consecutive orientations was greater than 45° or the FA value was smaller than 0.15. If a fiber seeding from a voxel in one node succeeded tracking to another node (i.e., terminating in any voxel in the other node), the two nodes would be considered connected by this tracking path. The mean FA value of all fibers connecting these two nodes was considered as the strength value of the connection between the nodes. In this case, the maximal possible number of connections between the 90 nodes in a network was 4,005.

Investigation of the alterations in the global properties in the SD network

To determine whether SD disrupts the healthy structural network, we compared the global network attributes of whole-brain networks between the SD and healthy groups. Small-world attributes have been widely used to depict the topological properties of networks [37, 38]. There are two common small-world measures, i.e., γ and λ , which represent the local and global efficiencies in a given network, respectively. These measures are calculated using the following formula: $\gamma = C^{\text{real}} / C^{\text{rand}}$ and $\lambda = L^{\text{real}} / L^{\text{rand}}$, where C^{real} and L^{real} are the observed clustering coefficient and characteristic path of brain networks, and C^{rand} and L^{rand} are the corresponding measurements of 10,000 random networks preserving the same number of nodes and edges and degree of distribution as a real network [39]. The cluster coefficient quantifies the connection density between the neighbors of a node ($C = \frac{1}{N} \sum_i \frac{E_i}{0.5 * k_i * (k_i - 1)}$). N is the number of nodes. E_i is the number of connections among the neighbors of node i . k_i is the number of neighbors of node i . The characteristic path is

the average of shortest path lengths between each node pair in the network ($L = \frac{1}{N*(N-1)} \sum_{i,j,i \neq j} d_{ij} \cdot N$ is the number of nodes. i and j are the node pair in the network. d_{ij} is the shortest path length between node i and j .) [35, 37, 40, 41]. In addition, other global network measures (i.e., mean network degree, assortativity and betweenness) used in previous studies [20, 35, 42] were also adopted in our study. The network degree is the average connectivity strength among all nodes. Assortativity is calculated by correlating the nodal degree and its neighbors' mean degree. High assortativity value implicates that the nodes are tightly connected. Network assortativity is the mean value of all nodes. Betweenness is the number of shortest paths through a node divided by the number of all possible shortest paths, indicating the influence of a node on a network. The network betweenness is the average value of all nodes [20, 35, 37, 43].

Using the above-mentioned methods, we calculated the two small-world measures (γ and λ) and three global measures (network degree, assortativity and betweenness) for each SD and healthy subject. These processes were completed using a graph theoretical network analysis toolbox for imaging connectomics (GRETNA) [44]. Then, two-sample t -tests were adopted to compare the measures between the subject groups.

Identification of modules in the structural network in SD

To determine whether the anatomical networks in the SD patients and healthy controls were organized into different modules and whether the modules had group difference, we conducted a modularity analysis on the mean network matrix of the two subject groups using the spectral optimization algorithm in GRETNA [44]. To avoid false-positive connections, the threshold was defined as $FA > 0.15$ for the mean networks of the SD patients and controls (see similar methods in Agosta et al. [20]) The number of modules in the network was determined by acquiring the maximal modularity Q , which represents a comparison of the within-module and inter-module connections [45]. To determine whether the Q value was significantly higher than that in the random networks, a Z score was calculated by dividing the Q value in the real network by the Q values generated from 10,000 random networks that preserve the same number of nodes and connections, and degree of distribution [39].

The distribution of the node number in different modules was assessed by a series of chi-square tests comparing the SD and control cohorts to determine whether there is significant difference between the SD and control groups. To investigate the damage of all modules, we first extracted the masks of GMV and diffusion metrics in each module. The GMV and diffusion masks were composed by the regions of the module in the AAL atlas and all white matter tracts in the module, respectively. Second, the modular GMV values were extracted by averaging GMV of all voxels in the masks. The 4 mean diffusion metrics of each module were computed by averaging the diffusion metrics of all voxels in the mask of the module and dividing by the number of possible connections of the module in all subjects. Third, we compared the GMV and diffusion metrics between the groups.

Identification of modules associated with semantic deficits in SD

To find which modules of SD observed in the above analyses were related with the semantic disruptions in SD, we calculated the correlation between the four diffusion metrics of each module and the semantic PCA scores across the 19 patients. To further determine whether the semantic-relevant effects of the modules observed in the above analyses were driven by other confounding variables, we carried out partial correlation analyses between the observed module's FA values and the semantic PCA scores by additionally partialling out the influence of the following potential confounding variables: (1) total GMV (GMV of all voxels in the whole-brain gray-matter mask), (2) modular GMV (GMV of all voxels in the mask of the corresponding module), (3) general cognitive state (the corrected t -score of the MMSE test), and (4) the atrophy lateralization (a dichotomic variable: left- or right-hemispheric predominate atrophy was coded as 1 or 0, respectively, see a similar method in Ding et al. [25]).

RESULTS

Neuropsychological and atrophy profiles of participants

Table 1 shows the demographic information, neuropsychological performance, and cerebral atrophy of the SD patients relative to those of the healthy subjects. There were no differences between these two groups in terms of the demographic

variables (p values >0.15). According to the raw accuracies, the SD patients exhibited an impaired semantic ability (t -values <-8.02 , p values <0.001), general cognitive ability ($t=-6.98$, $p<0.001$), and other cognitive abilities (word reading: $t=-4.97$, $p<0.001$; sound perception: $t=-3.45$, $p<0.002$; Rey-O recall: $t=-3.08$, $p<0.004$), but the abilities of oral repetition ($t=-0.65$, $p=0.52$), visual perception ($t=1.93$, $p=0.06$), sentence comprehension ($t=-1.11$, $p=0.28$), executive control ($t=1.46$, $p=0.16$), and arithmetic ($t=-1.49$, $p=0.15$) were spared. These results were also observed using the standardized t scores of the SD group. Moreover, the SD patients showed severe atrophy in the bilateral ATL and total GMV (t values >-4.55 , p values <0.001 ; Table 1), extending into other temporal and frontal areas (Fig. 2A; FDR corrected $p<0.05$). In total, 13 patients exhibited the left-hemispheric predominant atrophy.

The PCA analysis extracted three distinct components that accounted for 78% of the overall variance (i.e., component 1 = 47%, component 2 = 16%, and component 3 = 15%). The loading weights of all tasks on each component are listed in Table 2. Component 1 was treated as a semantic component since it had high loading weights on all semantic tasks (>0.61). Meanwhile, components 2 and 3 were treated as perceptual and arithmetic components because their heaviest loading weights were on the two perceptual tasks (>0.65) and proximity task (0.96), respectively.

Alterations in the global properties in the SD network

We found that the small-world attribute, i.e., the λ value, in the SD patients was significantly higher than that in the healthy subjects (SD: 1.08 ± 0.01 ; controls: 1.08 ± 0.01 ; $t=2.11$, $p<0.03$). However, the values of γ were comparable between the two groups (SD: 2.84 ± 0.28 ; controls: 2.70 ± 0.19 ; $t=1.84$, $p=0.07$). These findings demonstrate that the SD patients had a reduced global processing efficiency, but their local processing efficiency in the network was unaffected. We did not find any difference between the two cohorts in the other 3 global network measures (degree: $t=-1.3$, $p=0.20$; betweenness: $t=1.52$, $p=0.14$; assortativity: $t=0.43$, $p=0.67$).

Modules associated with semantic deficits in SD

When we used an FA value >0.15 as the threshold, the mean network densities in the SD patients and

controls were 0.14 and 0.15, respectively. For each subject group, our modularity analysis divided the 90 nodes into the following four modules (SD: $Q=0.47$, $Z=27.40$; controls: $Q=0.44$, $Z=24.64$; see Figs. 2 & 3): the left temporal/occipital/parietal module (SD: 17 nodes; controls: 22 nodes; $\chi^2=0.64$, $p=0.42$), the left frontal module (SD: 28 nodes; controls: 27 nodes; $\chi^2=0.02$, $p=0.89$), the right temporal/occipital module (SD: 22 nodes; controls: 23 nodes; $\chi^2=0.02$, $p=0.88$), and the right frontal/parietal module (SD: 23 nodes; controls: 18 nodes; $\chi^2=0.61$, $p=0.44$). The label of each node is presented in Table 3.

Seventy-four of the 90 nodes were divided into identical modules between the two groups. Relative to random level, the number of overlap nodes between the groups (74/90) was significantly higher than that at the random level (25%) ($\chi^2=157$, $p<0.001$), indicating that the SD patients had a module pattern in the node distribution that was highly similar to that in the controls. However, the gray-matter volumes of all modules were lower in the SD patients than those in controls (t -values <-2.74 , p -values <0.009). In contrast, SD disease led to an increase in the three white-matter integrity measures (i.e., MD, AD, and RD) in the left temporal/occipital/parietal module (t values >2.17 , p values <0.04) and the RD values in the right temporal/occipital module ($t=2.12$, $p=0.04$). No other group differences reached a significant level (t -values <1.86 or >-0.76 , p values >0.07).

Figure 3 displays the correlations between the diffusion metrics in each module and the semantic PCA scores in the SD individuals. Significantly positive correlations were observed in the left temporal/occipital/parietal module in all metrics (r values >0.54 , p values <0.02) and in the right frontal/parietal module in the RD values ($r=0.46$, $p=0.05$). However, a negative correlation was observed in the left frontal module in the FA value ($r=-0.50$, $p<0.03$). Other correlations were not significant (r values <0.44 or >-0.34 , p values <0.06).

Importantly, the correlation between damage to the left frontal module and the semantic impairments remained significant even after controlling for the total GMV, modular GMV, general cognitive state, and atrophy lateralization (partial r -values <-0.52 , p -values <0.03). Similarly, the effects in the left temporal/occipital/parietal module remained significant or marginally significant after controlling for all of the above-mentioned confounding factors (r values >0.41 , p values <0.09) except for the modular GMV (r values <0.22 , p values >0.38). Note that the GMV values in this module were significantly

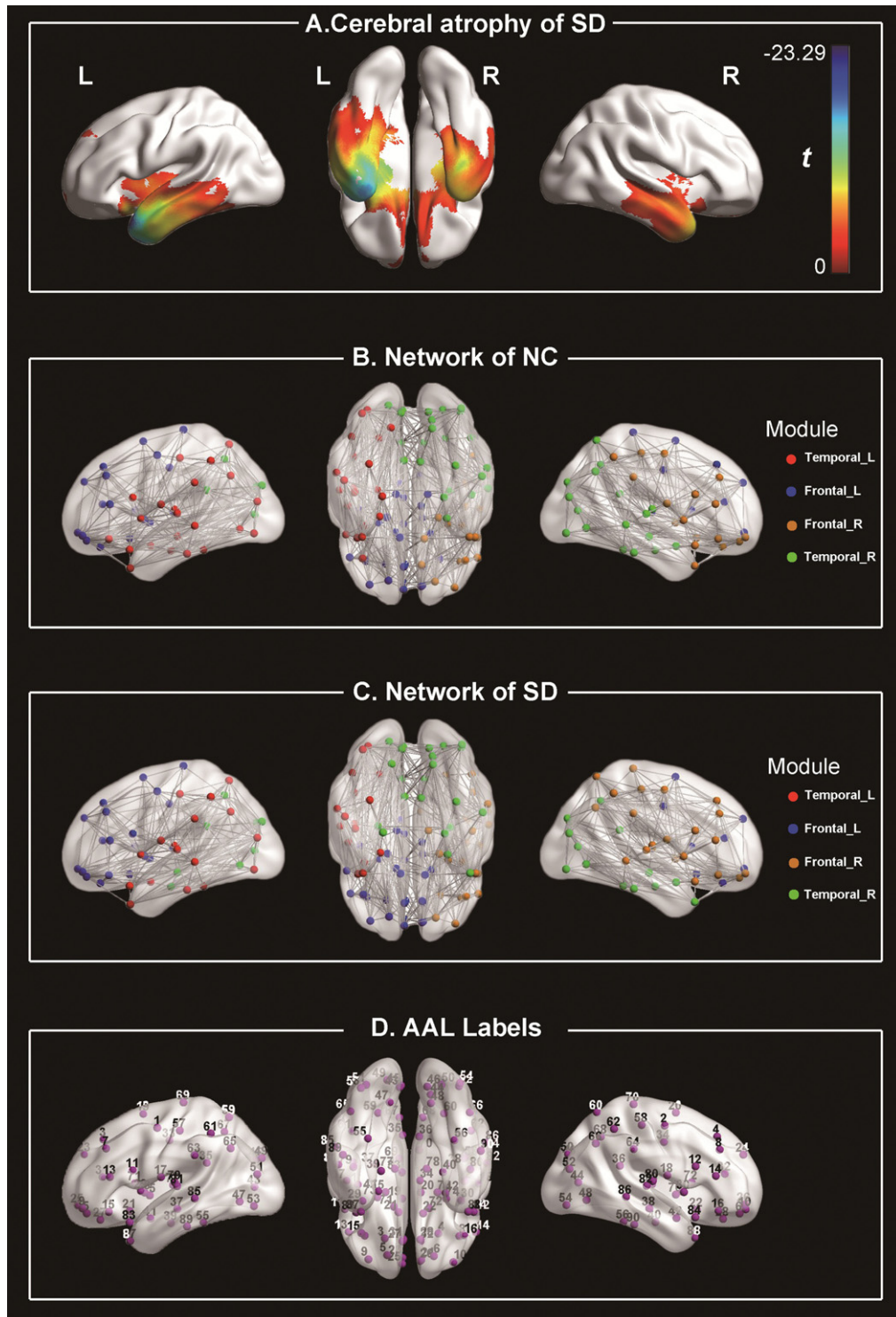


Fig. 2. Atrophy pattern in the SD patients and white-matter networks in the normal control and SD groups. Panel A shows the cerebral atrophy in SD (FDR corrected $p < 0.05$). Panels B and C denote the modular and connectivity pattern in SD and NC. Panel D shows the labels of the regions, and their corresponding names are provided in Table 3. NC, normal controls; SD, semantic dementia; Temporal_L, left temporal/occipital/parietal module; Frontal_L, left frontal module; Frontal_R, right frontal/parietal module; Temporal_R, right temporal/occipital module.

Table 2
Loading weights of each task on each component in principle component analysis

Tasks	Semantic component	Perceptual component	Arithmetic component
Word picture verification	0.80	0.45	0.06
Picture associative matching	0.61	0.51	0.01
Word associative matching	0.73	0.28	0.45
Oral picture naming	0.95	-0.02	0.08
Naming to definition	0.89	-0.07	-0.09
Sound naming	0.84	-0.04	-0.10
Visual perception	-0.15	0.81	-0.39
Sound perception	0.13	0.65	0.31
Proximity judgment	-0.09	-0.03	0.96

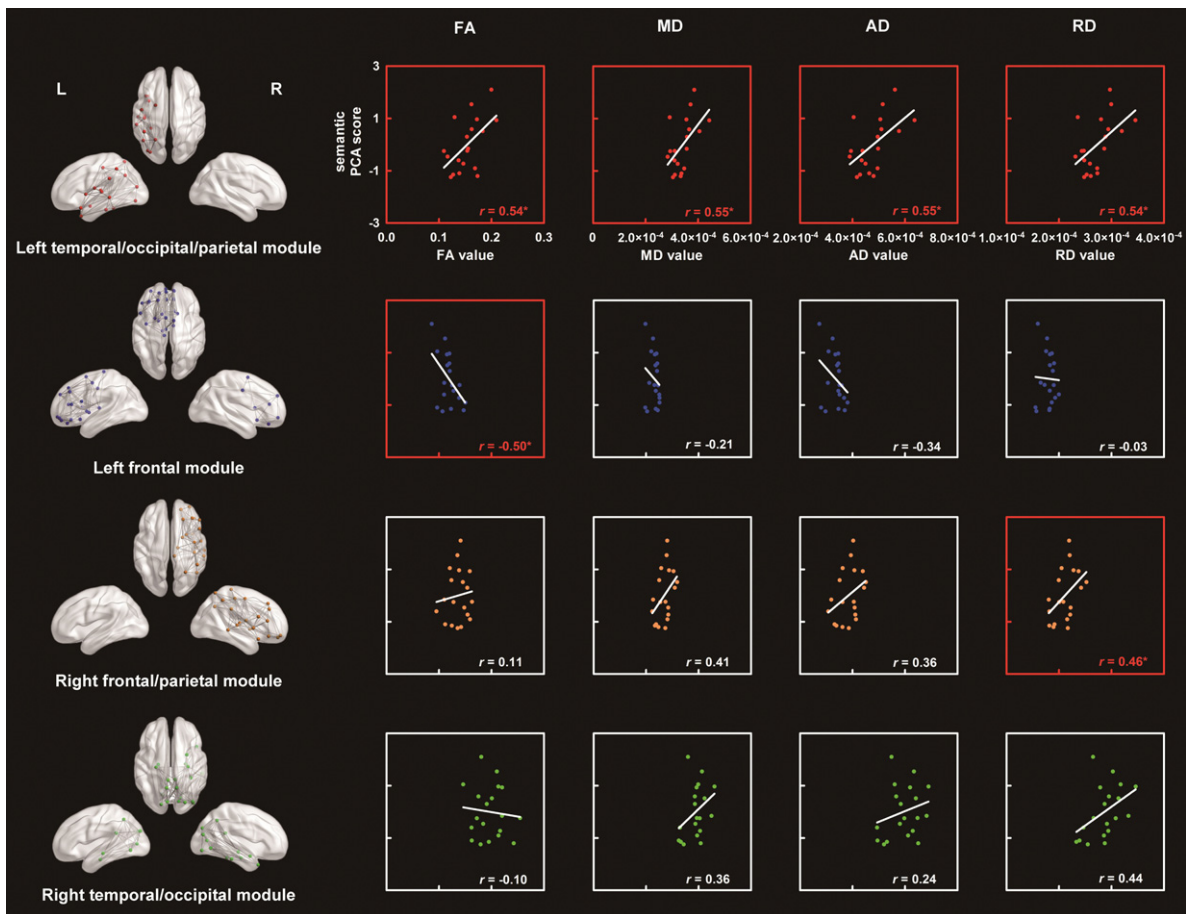


Fig. 3. Four modules in the SD white-matter network and the correlations between the diffusion metrics of each module and the semantic performance in the SD patients. The labels and names of the nodes in each module are provided in Fig. 2D and Table 3, respectively. * $p < 0.05$. FA, fractional anisotropy; MD, mean diffusivity; AD, axial diffusivity; RD, radial diffusivity; PCA, principle component analysis.

correlated with the semantic impairments in the SD patients ($r = 0.73$, $p = 0.004$). This finding suggests that the gray matter in this module might be involved in semantic processing. The effects of the right frontal/parietal module could not be accounted

for by all confounding factors (r values > 0.44 , p values < 0.07) except for the total volume ($r = 0.37$, $p = 0.13$). Moreover, the GMV values of the module were associated with the raw scores of the shape trail test ($r = -0.58$, $p = 0.02$), indicating that

Table 3
The distribution of the 90 AAL regions in the four modules in the white-matter network in SD

Label	Name	Module	Label	Name	Module
1	Precentral_L	Frontal_L	46	Cuneus_R	Temporal_R
2	Precentral_R	Frontal_R	47	Lingual_L	Temporal_R
3	Frontal_Sup_L	Frontal_L	48	Lingual_R	Temporal_R
4	Frontal_Sup_R	Frontal_R	49	Occipital_Sup_L	Temporal_R
5	Frontal_Sup_Orb_L	Frontal_L	50	Occipital_Sup_R	Temporal_R
6	Frontal_Sup_Orb_R	Frontal_R	51	Occipital_Mid_L	Temporal_L
7	Frontal_Mid_L	Frontal_L	52	Occipital_Mid_R	Temporal_R
8	Frontal_Mid_R	Frontal_R	53	Occipital_Inf_L	Temporal_L
9	Frontal_Mid_Orb_L	Frontal_L	54	Occipital_Inf_R	Temporal_L
10	Frontal_Mid_Orb_R	Frontal_R	55	Fusiform_L	Temporal_L
11	Frontal_Inf_Oper_L	Frontal_L	56	Fusiform_R	Temporal_R
12	Frontal_Inf_Oper_R	Frontal_R	57	Postcentral_L	Temporal_L
13	Frontal_Inf_Tri_L	Frontal_L	58	Postcentral_R	Frontal_R
14	Frontal_Inf_Tri_R	Frontal_R	59	Parietal_Sup_L	Temporal_L
15	Frontal_Inf_Orb_L	Frontal_L	60	Parietal_Sup_R	Frontal_R
16	Frontal_Inf_Orb_R	Frontal_R	61	Parietal_Inf_L	Temporal_L
17	Rolandic_Oper_L	Temporal_L	62	Parietal_Inf_R	Frontal_R
18	Rolandic_Oper_R	Frontal_R	63	SupraMarginal_L	Temporal_L
19	Supp_Motor_Area_L	Frontal_L	64	SupraMarginal_R	Frontal_R
20	Supp_Motor_Area_R	Frontal_L	65	Angular_L	Temporal_L
21	Olfactory_L	Frontal_L	66	Angular_R	Frontal_R
22	Olfactory_R	Frontal_L	67	Precuneus_L	Temporal_R
23	Frontal_Sup_Medial_L	Frontal_L	68	Precuneus_R	Temporal_R
24	Frontal_Sup_Medial_R	Frontal_L	69	Paracentral_Lobule_L	Frontal_L
25	Frontal_Mid_Orb_L	Frontal_L	70	Paracentral_Lobule_R	Frontal_R
26	Frontal_Mid_Orb_R	Frontal_L	71	Caudate_L	Frontal_L
27	Rectus_L	Frontal_L	72	Caudate_R	Frontal_L
28	Rectus_R	Frontal_L	73	Putamen_L	Frontal_L
29	Insula_L	Temporal_L	74	Putamen_R	Frontal_R
30	Insula_R	Frontal_R	75	Pallidum_L	Frontal_L
31	Cingulum_Ant_L	Frontal_L	76	Pallidum_R	Frontal_R
32	Cingulum_Ant_R	Frontal_L	77	Thalamus_L	Frontal_L
33	Cingulum_Mid_L	Frontal_L	78	Thalamus_R	Frontal_R
34	Cingulum_Mid_R	Frontal_L	79	Heschl_L	Temporal_L
35	Cingulum_Post_L	Temporal_R	80	Heschl_R	Frontal_R
36	Cingulum_Post_R	Temporal_R	81	Temporal_Sup_L	Temporal_L
37	Hippocampus_L	Temporal_R	82	Temporal_Sup_R	Frontal_R
38	Hippocampus_R	Temporal_R	83	Temporal_Pole_Sup_L	Temporal_L
39	ParaHippocampal_L	Temporal_R	84	Temporal_Pole_Sup_R	Frontal_R
40	ParaHippocampal_R	Temporal_R	85	Temporal_Mid_L	Temporal_L
41	Amygdala_L	Temporal_L	86	Temporal_Mid_R	Frontal_R
42	Amygdala_R	Temporal_R	87	Temporal_Pole_Mid_L	Temporal_L
43	Calcarine_L	Temporal_R	88	Temporal_Pole_Mid_R	Temporal_R
44	Calcarine_R	Temporal_R	89	Temporal_Inf_L	Temporal_L
45	Cuneus_L	Temporal_R	90	Temporal_Inf_R	Temporal_R

Temporal_L, left temporal/occipital/parietal module; Frontal_L, left frontal module; Temporal_R, right temporal/occipital module; Frontal_R, right frontal/parietal module; Ant, anterior; Inf, inferior; L, left; Med, medial; Mid, middle; Oper, opercularis; Orb, orbital; Post, posterior; R, right; Sup, superior; Supp, supplementary; Tri, triangularis.

this module might be engaged in general executive control.

DISCUSSION

SD is a disorder characterized by selective semantic deficits due to brain atrophy; thus, SD has become an ideal lesion model to explore the neural basis of semantic processing. This study aimed to investigate

the topological global attributes and semantic-deficit-relevant modules in the neuroanatomical network of SD patients. We observed that the network had an increased characteristic path length and was split into four distinct modules (left temporal/occipital/parietal, frontal, right frontal/parietal, and temporal/occipital modules). The first two modules were related to the semantic decline of this disease. The third module was involved in general cognitive control.

The global topological changes in the white-matter network of SD

We observed that the anatomical network in the SD subjects relative to that in the healthy controls had an increased λ value but no significant differences in γ or the other global network measures (degree, betweenness, and assortativity). This finding indicates that SD patients show a declined global efficiency with spared local efficiency. The two efficiencies reflect the different properties of a network. The global efficiency refers to the ability to transform information between any two nodes in the network and can be measured by the characteristic path length (λ value). The global efficiency mainly relies on the edges connecting far-distance nodes. In contrast, the local efficiency represents the ability to transform information between neighbor nodes, which can be measured by the cluster coefficient. The local efficiency mainly depends on the strength of local connections [38, 41]. Thus, our results indicate that distant white-matter pathways in the SD network are disrupted but the local white-matter tracts remain intact. This brain network pattern satisfies the deterioration rules in degenerative diseases [42]. Notably, Agosta et al. [15] also found that SD altered other global network measures (e.g., degree and assortativity) in the functional network. However, a similar pattern was not observed in our study. This difference might be due to the following differences between the two studies. One difference is the type of neural network type (functional versus structural network). The changes in SD might occur earlier in a functional network than in a structural network [46] or the brain atrophy might be more severe in a gray-matter network than in a white-matter network [47]. Therefore, the functional gray-matter network reported by Agosta et al. [20] presented more alterations than the structural white-matter network presented in our study. Other possible reasons include differences in the number of patients (13 versus 19) or brain lesion types (patients with predominant atrophy only in the left hemisphere versus those with predominant atrophy in the left and right hemispheres).

The semantic deficit-relevant modules in the SD network

We found that the anatomical network in SD could be divided into four independent modules. The modular patterns were quite similar in the SD and control groups, although there was reduced gray-matter atrophy in all the modules and significant

white-matter changes in the left and right temporal/occipital modules of the SD patients. Moreover, the abnormalities in three modules (i.e., the left temporal/occipital/parietal module, the left frontal module, the right frontal/parietal module) were correlated with the semantic impairments in the SD patients. We speculate that the left temporal/occipital/parietal and frontal modules might be dedicated to the following critical components of semantic cognition: semantic representation and control, respectively [48–50]. However, the right frontal/parietal module might be crucial for general executive control.

Comparisons between the SD and control groups

The modular patterns in the SD patients and controls were highly similar, suggesting that the brain atrophy in the SD patients did not affect the whole structural connectivity pattern. However, all modules showed significant changes in the gray-matter volumes, indicating that the nodes were damaged. In contrast, the white-matter changes only occurred in the left and right temporal/occipital modules, suggesting relatively circumscribed damage in the white matter.

The left temporal/occipital/parietal module

This module consists of multiple gray-matter regions and white-matter tracts in the left temporal, occipital and parietal lobes (Fig. 3). We found a significantly positive correlation between its mean FA, AD, RD, and MD values and the semantic deficit severity in the SD group, indicating that the damage in this module could lead to the deterioration of semantic processing in the patients.

Semantic cognition is underpinned by two following main components: semantic representation and control. Semantic representation integrates information from various sensorimotor modalities and forms semantic knowledge. This process is thought to be reliant on the ATL (a node within the module) [3]. Previous studies have found that the ATL has considerable structural and functional connections with other modality-specific and semantic-related areas [51, 52]. A dysfunction of this region results in disorders involving semantic tasks [53, 54] and shows strong effects on familiarity, item consistency, and task correlations in SD patients [55]. Using a computational model, Rogers and colleagues [4] confirmed the vital role of the ATL in semantic representation and successfully predicted the symptom pattern in SD. Moreover, Whitney and colleagues [56] found that the ATL was activated in tasks

involving the retrieval of word meaning after controlling for executive demands. Some studies also suggest that conceptual object properties are represented in the ATL [57, 58]. The module also includes other semantic-relevant regions or tracts. For instance, the fusiform gyrus is related to the semantic deficits in SD [8, 25]. The inferior fronto-occipital fasciculus connecting the frontal and occipital lobes is also relevant to semantic processing in both the patient and control cohorts [29, 59, 60]. Altogether, we speculate that the left ventral module plays a significant role in semantic representation, and its dysfunction results in a semantic processing inability.

Notably, the gray-matter volume in the module can also account for the variance in the semantic deterioration in SD, indicating that the white- and gray-matter in this module may both play an important role in semantic processing.

The left frontal module

Most of the nodes in the module were located in the left frontal lobe, and the other nodes were located in the right medial frontal lobe. Unexpectedly, what we observed was a robust negative correlation between the mean FA values in this module and the semantic scores of the SD subjects. This result likely occurred because, as a semantic control module, the left dorsal module plays a compensatory role in semantic representational deficits of SD. A compensatory mechanism is characterized by a greater response or a higher connectivity of potential cortical regions in a disease state relative to that in a healthy condition [61].

Semantic control is a part of semantic processing that engages in the monitoring, selection, and inhibition of semantic knowledge regardless of the modality of the input [48, 50]. Jefferies [48] identified the brain regions specific to semantic control, including the left inferior frontal gyrus, angular gyrus, and posterior middle temporal lobes. The left inferior frontal gyrus was included in the module. This region was activated in semantic tasks with strong selection demands [62]. A temporary dysfunction in this region only disrupted semantic tasks with high-control demands [63]. Patients with damage to this area were sensitive to the task difficulty but not to the familiarity or item consistency [55]. Other regions in this module have also been reported to execute a control function in semantic tasks (which may not be specific to semantic control). For instance, the dorso-lateral prefrontal cortex is involved in highly difficult semantic tasks [64]. Binder et al. [65] speculated

that the medial ventral and dorsal frontal areas were involved in emotional semantic processing and specific control, respectively. These two regions are also a part of the default mode network [66], which has been thought to engage in semantic processing [67]. In addition, the bilateral anterior cingulate cortices are also postulated as regions involved in semantic control [68, 69]. Overall, we propose that this module compensates for the deficits in semantic representation by increasing the control level. This hypothesis is consistent with the findings that there is hyperconnectivity in the prefrontal network of SD subjects [23] and an increased prefrontal activity for executive control tasks has been found in AD patients [70].

The right frontal/parietal module

This module includes most of the right frontal and parietal regions. Its RD values were positively correlated with the severity of the semantic impairments in SD. However, this correlation became insignificant when the total gray-matter volume was excluded. In addition, its RD values were also correlated with the scores of shape trail test. This finding suggests that this module contributes to general cognitive processing.

Limitations

This study has some caveats as follows: (1) We only inspected the general semantic processing ability in SD subjects, but the finer semantic processing abilities (e.g., different categories or modalities [71, 72]) were not investigated. (2) We recruited an unequal number of SD patients with left and right dominant atrophy. This uneven sample may have led us to miss the effect of right temporal modules in semantic processing, because the semantic system is thought to depend on both hemispheres [50]. (3) The subject number was relatively low for the PCA analysis. (4) Some of our cognitive assessments were developed in house. (5) The influence of the fiber crossing on the white-matter integrity values (e.g., FA value) was not considered. (6) Our brain gray-matter template is not a good representation of functional regions. (7) Because the atrophy of patients did not affect all regions in the modules, the effect of the modules might be associative with only part of the modules.

Conclusion

After constructing the whole-brain neuroanatomical network of SD, we observed that the network

had a decreased global efficiency. The network was separated into the following distinct modules: left temporal/occipital/parietal, frontal, right frontal/parietal and temporal/occipital modules. The first two modules were associated with the semantic deficits in SD. The third module might be crucial for general executive control. These findings can deepen our understanding of the structure of the SD neural network, which may have important clinical implications for the treatment of this disease.

ACKNOWLEDGMENTS

We are grateful to all research participants for their patience. This work was supported by the 973 Program (2014CB846100), the National Natural Science Foundation of China (81171019, 31271115), the Major Project of National Social Science Foundation (13&ZD188), and the Fundamental Research Funds for the Central Universities (2017XTCX04).

Authors' disclosures available online (<http://j-alz.com/manuscript-disclosures/17-0449r1>).

REFERENCES

- [1] Tulving E (1986) Episodic and semantic memory: Where should we go from here? *Behav Brain Sci* **9**, 573-577.
- [2] Goll JC, Ridgway GR, Crutch SJ, Theunissen FE, Warren JD (2012) Nonverbal sound processing in semantic dementia: A functional MRI study. *Neuroimage* **61**, 170-180.
- [3] Patterson K, Nestor PJ, Rogers TT (2007) Where do you know what you know? The representation of semantic knowledge in the human brain. *Nat Rev Neurosci* **8**, 976-987.
- [4] Rogers TT, Lambon Ralph MA, Garrard P, Bozeat S, McClelland JL, Hodges JR, Patterson K (2004) Structure and deterioration of semantic memory: A neuropsychological and computational investigation. *Psychol Rev* **111**, 205-235.
- [5] Lambon Ralph MA, Graham KS, Patterson K, Hodges JR (1999) Is a picture worth a thousand words? Evidence from concept definitions by patients with semantic dementia. *Brain Lang* **70**, 309-335.
- [6] Agosta F, Henry RG, Migliaccio R, Neuhaus J, Miller BL, Dronkers NF, Brambati SM, Filippi M, Ogar JM, Wilson SM, Gorno-Tempini ML (2010) Language networks in semantic dementia. *Brain* **133**, 286-299.
- [7] Wilson SM, DeMarco AT, Henry ML, Gesierich B, Babiak M, Mandelli ML, Miller BL, Gorno-Tempini ML (2014) What role does the anterior temporal lobe play in sentence-level processing? Neural correlates of syntactic processing in semantic variant primary progressive aphasia. *J Cogn Neurosci* **26**, 970-985.
- [8] Mion M, Patterson K, Acosta-Cabronero J, Pengas G, Izquierdo-Garcia D, Hong YT, Fryer TD, Williams GB, Hodges JR, Nestor PJ (2010) What the left and right anterior fusiform gyri tell us about semantic memory. *Brain* **133**, 3256-3268.
- [9] Mummery CJ, Patterson K, Price C, Ashburner J, Frackowiak RS, Hodges JR (2000) A voxel-based morphometry study of semantic dementia: Relationship between temporal lobe atrophy and semantic memory. *Ann Neurol* **47**, 36-45.
- [10] Acosta-Cabronero J, Patterson K, Fryer TD, Hodges JR, Pengas G, Williams GB, Nestor PJ (2011) Atrophy, hypometabolism and white matter abnormalities in semantic dementia tell a coherent story. *Brain* **134**, 2025-2035.
- [11] Guo CC, Gorno-Tempini ML, Gesierich B, Henry M, Trujillo A, Shany-Ur T, Jovicich J, Robinson SD, Kramer JH, Rankin KP, Miller BL, Seeley WW (2013) Anterior temporal lobe degeneration produces widespread network-driven dysfunction. *Brain* **136**, 2979-2991.
- [12] Seeley WW, Crawford RK, Zhou J, Miller BL, Greicius MD (2009) Neurodegenerative diseases target large-scale human brain networks. *Neuron* **62**, 42-52.
- [13] La Joie R, Landeau B, Perrotin A, Bejanin A, Egret S, Pélerin A, Mézenge F, Belliard S, de La Sayette V, Eustache F, Desgranges B, Chételat G (2014) Intrinsic connectivity identifies the hippocampus as a main crossroad between Alzheimer's and semantic dementia-targeted networks. *Neuron* **81**, 1417-1428.
- [14] Agosta F, Galantucci S, Canu E, Cappa SF, Magnani G, Franceschi M, Falini A, Comi G, Filippi M (2013) Disruption of structural connectivity along the dorsal and ventral language pathways in patients with nonfluent and semantic variant primary progressive aphasia: A DT MRI study and a literature review. *Brain Lang* **127**, 157-166.
- [15] Schwindt GC, Graham NL, Rochon E, Tang-Wai DF, Lobaugh NJ, Chow TW, Black SE (2013) Whole-brain white matter disruption in semantic and nonfluent variants of primary progressive aphasia. *Hum Brain Mapp* **34**, 973-984.
- [16] Binney RJ, Parker GJ, Lambon Ralph MA (2012) Convergent connectivity and graded specialization in the rostral human temporal lobe as revealed by diffusion-weighted imaging probabilistic tractography. *J Cogn Neurosci* **24**, 1998-2014.
- [17] Davey J, Thompson HE, Hallam G, Karapanagiotidis T, Murphy C, De Caso I, Krieger-Redwood K, Bernhardt BC, Smallwood J, Jefferies E (2016) Exploring the role of the posterior middle temporal gyrus in semantic cognition: Integration of anterior temporal lobe with executive processes. *Neuroimage* **137**, 165-177.
- [18] Hurley RS, Bonakdarpour B, Wang X, Mesulam MM (2015) Asymmetric connectivity between the anterior temporal lobe and the language network. *J Cogn Neurosci* **27**, 464-473.
- [19] Jackson RL, Hoffman P, Pobric G, Lambon Ralph MA (2016) The semantic network at work and rest: Differential connectivity of anterior temporal lobe subregions. *J Neurosci* **36**, 1490-1501.
- [20] Agosta F, Galantucci S, Valsasina P, Canu E, Meani A, Marccone A, Magnani G, Falini A, Comi G, Filippi M (2014) Disrupted brain connectome in semantic variant of primary progressive aphasia. *Neurobiol Aging* **35**, 2646-2655.
- [21] Hagmann P, Cammoun L, Gigandet X, Meuli R, Honey CJ, Wedeen VJ, Sporns O (2008) Mapping the structural core of human cerebral cortex. *PLoS Biol* **6**, e159.
- [22] Yeo BT, Krienen FM, Sepulcre J, Sabuncu MR, Lashkari D, Hollinshead M, Roffman JL, Smoller JW, Zöllei L, Polimeni JR, Fischl B, Liu H, Buckner RL (2011) The organization of the human cerebral cortex estimated by intrinsic functional connectivity. *J Neurophysiol* **106**, 1125-1165.

- [23] Farb NA, Grady CL, Strother S, Tang-Wai DF, Masellis M, Black S, Freedman M, Pollock BG, Campbell KL, Hasher L, Chow TW (2013) Abnormal network connectivity in frontotemporal dementia: Evidence for prefrontal isolation. *Cortex* **49**, 1856-1873.
- [24] Oldfield RC (1971) The assessment and analysis of handedness: The Edinburgh inventory. *Neuropsychologia* **9**, 97-113.
- [25] Ding J, Chen K, Chen Y, Fang Y, Yang Q, Lv Y, Lin N, Bi Y, Guo Q, Han Z (2016) The left fusiform gyrus is a critical region contributing to the core behavioral profile of semantic dementia. *Front Hum Neurosci* **10**, 215.
- [26] Gorno-Tempini ML, Hillis AE, Weintraub S, Kertesz A, Mendez M, Cappa SF, Ogar JM, Rohrer JD, Black S, Boeve BF, Manes F, Dronkers NF, Vandenberghe R, Rascovsky K, Patterson K, Miller BL, Knopman DS, Hodges JR, Mesulam MM, Grossman M (2011) Classification of primary progressive aphasia and its variants. *Neurology* **76**, 1006-1014.
- [27] Folstein MF, Folstein SE, McHugh PR (1975) "Minimal state". A practical method for grading the cognitive state of patients for the clinician. *J Psychiatr Res* **12**, 189-198.
- [28] Crawford JR, Garthwaite PH (2006) Comparing patients' predicted test scores from a regression equation with their obtained scores: A significance test and point estimate of abnormality with accompanying confidence limits. *Neuropsychology* **20**, 259-271.
- [29] Han Z, Ma Y, Gong G, He Y, Caramazza A, Bi Y (2013) White matter structural connectivity underlying semantic processing: Evidence from brain damaged patients. *Brain* **136**, 2952-2965.
- [30] Iuculano T, Tang J, Hall CW, Butterworth B (2008) Core information processing deficits in developmental dyscalculia and low numeracy. *Dev Sci* **11**, 669-680.
- [31] Cui Z, Zhong S, Xu P, He Y, Gong G (2013) PANDA: A pipeline toolbox for analyzing brain diffusion images. *Front Hum Neurosci* **7**, 42.
- [32] Jellison BJ, Field AS, Medow J, Lazar M, Salamat MS, Alexander AL (2004) Diffusion tensor imaging of cerebral white matter: A pictorial review of physics, fiber tract anatomy, and tumor imaging patterns. *AJNR Am J Neuroradiol* **25**, 356-369.
- [33] Jones DK (2008) Studying connections in the living human brain with diffusion MRI. *Cortex* **44**, 936-952.
- [34] Tzourio-Mazoyer N, Landeau B, Papathanassiou D, Crivello F, Etard O, Delcroix N, Mazoyer B, Joliot M (2002) Automated anatomical labeling of activations in SPM using a macroscopic anatomical parcellation of the MNI MRI single-subject brain. *Neuroimage* **15**, 273-289.
- [35] Gong G, He Y, Concha L, Lebel C, Gross DW, Evans AC, Beaulieu C (2009) Mapping anatomical connectivity patterns of human cerebral cortex using in vivo diffusion tensor imaging tractography. *Cereb Cortex* **19**, 524-536.
- [36] Mori S, Crain BJ, Chacko V, van Zijl P (1999) Three-dimensional tracking of axonal projections in the brain by magnetic resonance imaging. *Ann Neurol* **45**, 265-269.
- [37] Bullmore E, Sporns O (2009) Complex brain networks: Graph theoretical analysis of structural and functional systems. *Nat Rev Neurosci* **10**, 186-198.
- [38] Humphries MD, Gurney K, Prescott TJ (2006) The brainstem reticular formation is a small-world, not scale-free, network. *Proc Biol Sci* **273**, 503-511.
- [39] Maslov S, Sneppen K (2002) Specificity and stability in topology of protein networks. *Science* **296**, 910-913.
- [40] Latora V, Marchiori M (2001) Efficient behavior of small-world networks. *Phys Rev Lett* **87**, 198701.
- [41] Watts DJ, Strogatz SH (1998) Collective dynamics of 'small-world' networks. *Nature* **393**, 440-442.
- [42] Dai Z, Yan C, Li K, Wang Z, Wang J, Cao M, Lin Q, Shu N, Xia M, Bi Y, He Y (2015) Identifying and mapping connectivity patterns of brain network hubs in Alzheimer's disease. *Cereb Cortex* **25**, 3723-3742.
- [43] Newman ME (2003) The structure and function of complex networks. *SIAM Rev* **45**, 167-256.
- [44] Wang J, Wang X, Xia M, Liao X, Evans A, He Y (2015) GREYNA: A graph theoretical network analysis toolbox for imaging connectomics. *Front Hum Neurosci* **9**, 386.
- [45] Newman ME, Girvan M (2004) Finding and evaluating community structure in networks. *Phys Rev E Stat Nonlin Soft Matter Phys* **69**, 026113.
- [46] Uddin LQ (2013) Complex relationships between structural and functional brain connectivity. *Trends Cogn Sci* **17**, 600-602.
- [47] Hodges JR, Patterson K (2007) Semantic dementia: A unique clinicopathological syndrome. *Lancet Neurol* **6**, 1004-1014.
- [48] Jefferies E (2013) The neural basis of semantic cognition: Converging evidence from neuropsychology, neuroimaging and TMS. *Cortex* **49**, 611-625.
- [49] Warrington EK, McCarthy R (1983) Category specific access dysphasia. *Brain* **106**, 859-878.
- [50] Lambon Ralph MA, Jefferies E, Patterson K, Rogers TT (2017) The neural and computational bases of semantic cognition. *Nat Rev Neurosci* **18**, 42-55.
- [51] Fan L, Wang J, Zhang Y, Han W, Yu C, Jiang T (2014) Connectivity-based parcellation of the human temporal pole using diffusion tensor imaging. *Cereb Cortex* **24**, 3365-3378.
- [52] Pascual B, Masdeu JC, Hollenbeck M, Makris N, Insausti R, Ding SL, Dickerson BC (2015) Large-scale brain networks of the human left temporal pole: A functional connectivity MRI study. *Cereb Cortex* **25**, 680-702.
- [53] Pobric G, Jefferies E, Lambon Ralph MA (2010) Amodal semantic representations depend on both anterior temporal lobes: Evidence from repetitive transcranial magnetic stimulation. *Neuropsychologia* **48**, 1336-1342.
- [54] Pobric G, Jefferies E, Lambon Ralph MA (2007) Anterior temporal lobes mediate semantic representation: Mimicking semantic dementia by using rTMS in normal participants. *Proc Natl Acad Sci U S A* **104**, 20137-20141.
- [55] Jefferies E, Lambon Ralph MA (2006) Semantic impairment in stroke aphasia versus semantic dementia: A case-series comparison. *Brain* **129**, 2132-2147.
- [56] Whitney C, Jefferies E, Kircher T (2011) Heterogeneity of the left temporal lobe in semantic representation and control: Priming multiple versus single meanings of ambiguous words. *Cerebr Cortex* **21**, 831-844.
- [57] Peelen MV, Caramazza A (2012) Conceptual object representations in human anterior temporal cortex. *J Neurosci* **32**, 15728-15736.
- [58] Clarke A, Tyler LK (2014) Object-specific semantic coding in human perirhinal cortex. *J Neurosci* **34**, 4766-4775.
- [59] Nugiel T, Alm KH, Olson IR (2016) Individual differences in white matter microstructure predict semantic control. *Cogn Affect Behav Neurosci* **16**, 1003-1016.
- [60] Duffau H, Peggy Gatignol ST, Mandonnet E, Capelle L, Taillandier L (2008) Intraoperative subcortical stimulation mapping of language pathways in a consecutive series of

- 115 patients with Grade II glioma in the left dominant hemisphere. *J Neurosurg* **109**, 461-471.
- [61] Chen G, Zhang HY, Xie C, Chen G, Zhang ZJ, Teng GJ, Li SJ (2013) Modular reorganization of brain resting state networks and its independent validation in Alzheimer's disease patients. *Front Hum Neurosci* **7**, 456.
- [62] Thompson-Schill SL, D'Esposito M, Aguirre GK, Farah MJ (1997) Role of left inferior prefrontal cortex in retrieval of semantic knowledge: A reevaluation. *Proc Natl Acad Sci U S A* **94**, 14792-14797.
- [63] Whitney C, Kirk M, O'Sullivan J, Lambon Ralph MA, Jefferies E (2012) Executive semantic processing is underpinned by a large-scale neural network: Revealing the contribution of left prefrontal, posterior temporal, and parietal cortex to controlled retrieval and selection using TMS. *J Cogn Neurosci* **24**, 133-147.
- [64] Miotto EC, Savage CR, Evans JJ, Wilson BA, Martins M, Iaki S, Amaro E Jr (2006) Bilateral activation of the prefrontal cortex after strategic semantic cognitive training. *Hum Brain Mapp* **27**, 288-295.
- [65] Binder JR, Desai RH, Graves WW, Conant LL (2009) Where is the semantic system? A critical review and meta-analysis of 120 functional neuroimaging studies. *Cereb Cortex* **19**, 2767-2796.
- [66] Andrews-Hanna JR, Reidler JS, Sepulcre J, Poulin R, Buckner RL (2010) Functional-anatomic fractionation of the brain's default network. *Neuron* **65**, 550-562.
- [67] Binder JR, Desai RH (2011) The neurobiology of semantic memory. *Trends Cogn Sci* **15**, 527-536.
- [68] Zhao Y, Song L, Ding J, Lin N, Wang Q, Du X, Sun R, Han Z (2017) Left anterior temporal lobe and bilateral anterior cingulate cortex are semantic hub regions: Evidence from behavior-nodal degree mapping in brain-damaged patients. *J Neurosci* **37**, 141-151.
- [69] Duncan J (2010) The multiple-demand (MD) system of the primate brain: Mental programs for intelligent behaviour. *Trends Cogn Sci* **14**, 172-179.
- [70] Grady CL, McIntosh AR, Beig S, Keightley ML, Burian H, Black SE (2003) Evidence from functional neuroimaging of a compensatory prefrontal network in Alzheimer's disease. *J Neurosci* **23**, 986-993.
- [71] Butler CR, Brambati SM, Miller BL, Gorno-Tempini ML (2009) The neural correlates of verbal and nonverbal semantic processing deficits in neurodegenerative disease. *Cogn Behav Neurol* **22**, 73-80.
- [72] Pulvermüller F, Cooper-Pye E, Dine C, Hauk O, Nestor PJ, Patterson K (2010) The word processing deficit in semantic dementia: All categories are equal, but some categories are more equal than others. *J Cogn Neurosci* **22**, 2027-2041.